



Phase Diagram and Dielectric Studies in Hydrogen-Bonded Liquid Crystal System

E. I. Efremova, Z. A. Kydryashova, L. A. Nosikova, A. P. Kovshik, L. A. Dobrun & A. B. Melnikov

To cite this article: E. I. Efremova, Z. A. Kydryashova, L. A. Nosikova, A. P. Kovshik, L. A. Dobrun & A. B. Melnikov (2016) Phase Diagram and Dielectric Studies in Hydrogen-Bonded Liquid Crystal System, Molecular Crystals and Liquid Crystals, 626:1, 12-20, DOI: 10.1080/15421406.2015.1106220

To link to this article: <http://dx.doi.org/10.1080/15421406.2015.1106220>



Published online: 22 Mar 2016.



Submit your article to this journal [↗](#)



Article views: 79



View related articles [↗](#)



View Crossmark data [↗](#)

Phase Diagram and Dielectric Studies in Hydrogen-Bonded Liquid Crystal System

E. I. Efremova^a, Z. A. Kydryashova^{a,b}, L. A. Nosikova^{a,b}, A. P. Kovshik^c, L. A. Dobrun^c, and A. B. Melnikov^c

^aLomonosov Moscow State University of Fine Chemical Technologies, Prospect Vernadskogo 86, Moscow, Russia;

^bInstitute of Physical Chemistry and Electrochemistry, 31 Leninsky Prospect, Moscow, Russia; ^cSaint Petersburg State University, 7–9, Universitetskaya Nab, St. Petersburg, Russia

ABSTRACT



The thermal and dielectric behaviors of mixtures were investigated for systems of *p*-*n*-hexyloxybenzoic acid (**6OBA**) and *p*-*n*-octyloxybenzoic acid (**8OBA**) by differential scanning calorimetry, polarized optical microscopy, and dielectric measurements. The T-X phase diagram was obtained for this system. Eutectic composition was calculated and received experimentally. Enthalpies of mixing were calculated to describe phase transitions physically. All mixtures show enantiotropic smectic and nematic phases. Dielectric permittivity has higher value for the mixture with fractional proportion of 30 to 70% mol for **8OBA** than that for initial acid. It is assumed that co-crystallization of initial compound occurs when the ratio of components is close to equimolar ratio.

KEYWORDS

Dielectric measurement; intermolecular hydrogen bonding; phase diagram; *p*-*n*-alkoxybenzoic acids

1. Introduction

Hydrogen-bonding interaction plays a significant role in the molecular recognition and self-assembly of liquid crystalline phases. Rigid rod-shaped anisotropic molecules, appropriately functioned by recognizable moieties, interact in net or in solution and lead to the formation of supramolecular complexes that may exhibit thermotropic liquid crystalline character [1]. Basis of the development of the thermodynamics of liquid crystal (LC) state is the precision studies of phase transitions in mixtures of liquid crystals by means of thermal analysis and calorimetry [2]. Liquid crystals prepared by self-assembly processes via formation of intermolecular interactions, such as hydrogen bonding, are promising materials for fabrication of new functional materials [3]. Using *p*-*n*-alkoxybenzoic acids (AOBA) and their mixtures is very promising for creating liquid crystals with a predictable set of properties. These compounds exist as dimers, which are hydrogen-bonded. Dimerization of molecules dramatically changes the properties of liquid crystals and causes many interesting phenomena. The population of dimers usually depends on the surrounding conditions, such as temperature and external field, and therefore can be useful for the creation of sensing devices [4]. It has been earlier reported by Madhu Mohan and coauthors that these self-organized systems induce variety of new phenomena such as re-entrant phase occurrence [5–7], light modulation [8], optical shutter action [9, 10], and field-induced transitions [11]. Systems with AOBA have

CONTACT E. I. Efremova  katife2007@rambler.ru  Lomonosov Moscow State University of Fine Chemical Technologies, Prospect Vernadskogo 86, 119571 Moscow, Russia.

Color versions of one or more of the figures in the article can be found online at www.tandfonline.com/gmcl.

© 2016 Taylor & Francis Group, LLC

been found to exhibit a rich variety of frustrated smectic phases [12–15]. The actual task is to predict and create materials with predetermined parameters, so multi-component mixtures are used in practice based on an LC display (LCD) with H-bond. Construction of phase diagrams and the study of properties and dynamics of interaction of components and LC materials are important physicochemical basis for the development of science of liquid crystals [16]. AOBA is convenient for studying regularity of liquid crystals. It was chosen to create a model of obtaining new LC substances having a wider temperature range and stable mesophases. It would be suitable for other homologues of carboxylic acids.

The central theme of the present work is to study the physicochemical properties of supramolecular hydrogen-bonded liquid crystals formed by the blend of various combinations of AOBA through intermolecular hydrogen bonds. Phase behavior of binary system *p*-*n*-hexyloxybenzoic (**6OBA**)—*p*-*n*-heptyloxybenzoic (**7OBA**) acids was investigated by X-ray, dielectric, and volumetric measurements. Formation of new compounds with unique properties was observed at equimolar ratio in this system [17, 18]. The binary system of **7OBA** mixed in different ratios with *p*-*n*-undecyloxybenzoic acid (**11OBA**) shows extreme volume properties of **7OBA** and **11OBA** in 2:1 ratio [19, 20]. Formation of co-crystal was revealed by X-ray and dielectric measurements [21]. The present work is devoted to the study of thermodynamic characterization of binary mixtures of **6OBA** and *p*-*n*-octyloxybenzoic acid (**8OBA**). This system was investigated by polarized optical microscopy (POM), differential scanning calorimetry (DSC), and dielectric measurements. Investigations of dielectric properties provide a powerful tool to understand the structure–property relationship, which is essential not only from technological aspect but also to understand the basic science. Investigation of phenomenon of interactions in the systems of liquid crystals is paramount from both theoretical and practical standpoints [22]. Complete phase diagram (T-X) is constructed in the present work. The obtained results are also discussed.

2. Experimental

Optical textural observations were performed with Zeiss polarizing microscope equipped with Canon EOS 5D Mark II camera system with 2560×1920 -pixel resolution. Linkam THMS600 cell was used for studies at variable temperatures with precision of $\pm 0.1^\circ\text{C}$. Transition temperatures and corresponding enthalpy values were obtained by Differential Scanning Calorimeter Intec Q-100. The permittivity of the substances was measured by using Meter LCR HIOKI HiTESTER 3532–50 at 100 Hz–1 MHz frequency. The liquid crystals were oriented in a constant 5000-G magnetic field. A cell for permittivity measurements was a flat titanium capacitor, 250- μm thick, and temperature was controlled with a precision of 1°C . Permittivities were determined at a cell voltage of 1.2 V. The measurement error was 0.7%.

The starting analytic grade compounds were additionally purified by recrystallization from ethyl acetate. Mixtures of different concentrations were mixed thoroughly. The samples were homogenized above clearing point and then slowly cooled for 8–10 h. Phase composition of obtained mixtures is shown in Table 1.

3. Thermal and Thermodynamic Analysis

Thermal analysis showed that the initial components have the following phase transition temperature ($^\circ\text{C}$):

6OBA: Cr • 69.0°C • Cr • 105.0°C • N • 152.0°C • I

8OBA: Cr • 75.0°C • Cr • 101.0°C • SmC • 106.0°C • N • 148.0°C • I,

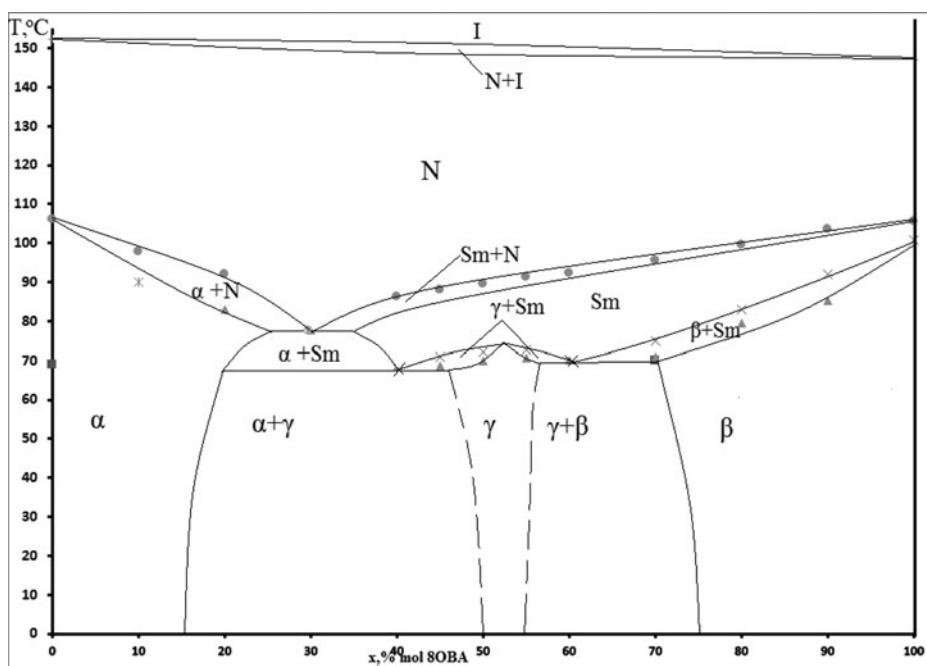


Figure 1. Phase diagram of system **6OBA–8OBA**.

where Cr = crystalline, Sm = smectic, N = nematic, I = isotropic phase. The mesogens of **6OBA** and **8OBA** are found to exhibit characteristic textures [23] of nematic (Schlieren brush texture of nematic phase) and smectic C (Schlieren texture) phases respectively. The general phase sequence of the system is:

$$\text{Cr} \leftrightarrow \text{SmC} \leftrightarrow \text{N} \leftrightarrow \text{I}.$$

The phase diagram of enantiotropic thermodynamically stable phase is shown in Fig. 1. Monotropic texture changes in mesophase, such as Sm X and polymorphic transitions during cooling, are not included due to their thermodynamic instability. The observed phase, transition temperatures, and corresponding enthalpy values obtained by DSC in the cooling and

Table 1. Transition temperature (°C) and corresponding enthalpy values (kJ/mol) obtained by DSC.

Number of sample	Mole fraction of 8OBA (%)	Phase transition (temperature (°C) and enthalpy values (kJ/mol))		
		Sm	N	I
8OBA	100	101.0 (12.5)	106 (0.5)	148.0 (3.5)
1	89	92.1 (6.4)	103.5 (1)	148 (2.5)
2	79	83 (7.1)	99.6 (1)	148.3 (3)
3	69	75.0 (8.8)	95.5 (1.1)	148.6 (2.6)
4	65	72.3 (8.6)	92.3 (1.1)	149.1 (2.9)
5	55	72.7 (9.2)	91.2 (1.1)	149.7 (2.7)
6	50	72.2 (8.6)	89.4 (1)	149.8 (2.85)
7	45	71 (8.6)	88.1 (1)	150.1 (3)
8	40	70.4 (7.9)	86.2 (1)	150.2 (2.9)
9	33	78 (7.9)	81 (1)	150.5 (2.9)
10	30	78 (8.4)	78 (1)	151.2 (2.9)
11	20	70 (5)	92.0 (8)	151.7 (2.9)
12	10		97.7 (10)	152.2 (2.6)
6OBA	0		105.0 (14.2)	152.0 (3.3)

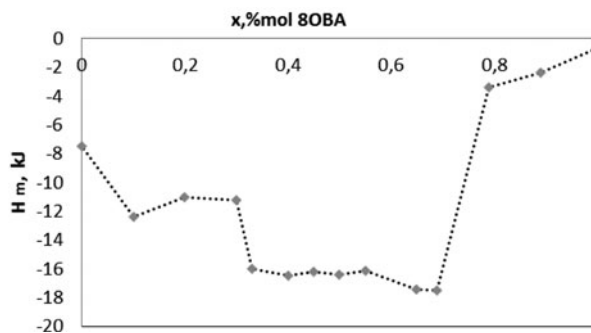


Figure 2. The mixing enthalpies as a function of composition in the system **6OBA–8OBA** for transition from crystal to liquid crystal.

heating cycles for the binary system are presented in Table 1. These data are in concurrence with the POM results.

Solid solutions are formed in the low temperature region of the system: α -region = solid solution based on **6OBA**, β -region = solid solution based on **8OBA**, and γ -region = co-crystallization of two acids by analogy with Efremova et al. [19, 21].

Acids dissolved partially with each other in the solid state. Phase transitions occur in the crystalline phase. It is associated with the polymorphism of initial components. **6OBA** and **8OBA** form a series of solid solutions based on initial components.

Determining the eutectic point theoretically, the Schroder–van Laar equations were used to predict eutectic temperatures and compositions [24]. The Schroder–van Laar equations are as follows: $T_i = \Delta H_f / (\Delta H_f / T_f) - R \ln x_i$. In the **6OBA–8OBA** system, X_e (experimental) = 40% mol **8OBA**, X_c (calculated) = 47% mol **8OBA** and T_e (experimental) = 72, T_c (calculated) = 70°C. The enthalpy of mixing for binary mixture is given by the following equation:

$$\Delta^M H = (\Delta^f H)_{\text{exp}} - \sum_i (x_i \Delta^f H_i^0), \quad (1)$$

where $(\Delta^f H)_{\text{exp}}$ is the experimental value of enthalpy of fusion, x_i and $\Delta^f H_i^0$ are mole fraction and enthalpy of fusion of component i respectively. The structure of binary mixtures depends on the sign and magnitude of enthalpy of mixing, therefore three types of structures are suggested [25]: quasi-eutectic for which $\Delta^M H > 0$; clustering of molecules, in which $\Delta^M H > 0$; and molecular solutions, for which $\Delta^M H = 0$. The dependence of the enthalpy of mixing as a function of the composition is shown in the Fig. 2. The thermodynamic properties of the **6OBA–8OBA** system differ greatly from those of an ideal system, although the dipole moments as well as the size and shape of molecules of both components are similar. The non-ideality of the system is indicated by the considerable values of $[\Delta^M H]$. The properties of the mixed phase of this system are mainly determined by energetic factors, in particular, by the character of electron density distribution in the molecules of asymmetric shape.

Non-ideal behavior of the **6OBA–8OBA** system may also be caused by a certain ability of each component to associate. In this case, we associate it with the formation of co-crystals at a ratio of components 50% mol of **8OBA**. In this work, the negative value of $\Delta^M H$ suggests the clustering of molecules in binary eutectic melt.

Crystalline transitions disappear for mixtures with compositions from 30 to 70% mol **6OBA**. This may be related to the conformational features taking place in this range. Co-crystallization is likely to have taken place in the region of γ , which is accompanied by a decrease in thermal effect. The system becomes less thermodynamically stable at a ratio close

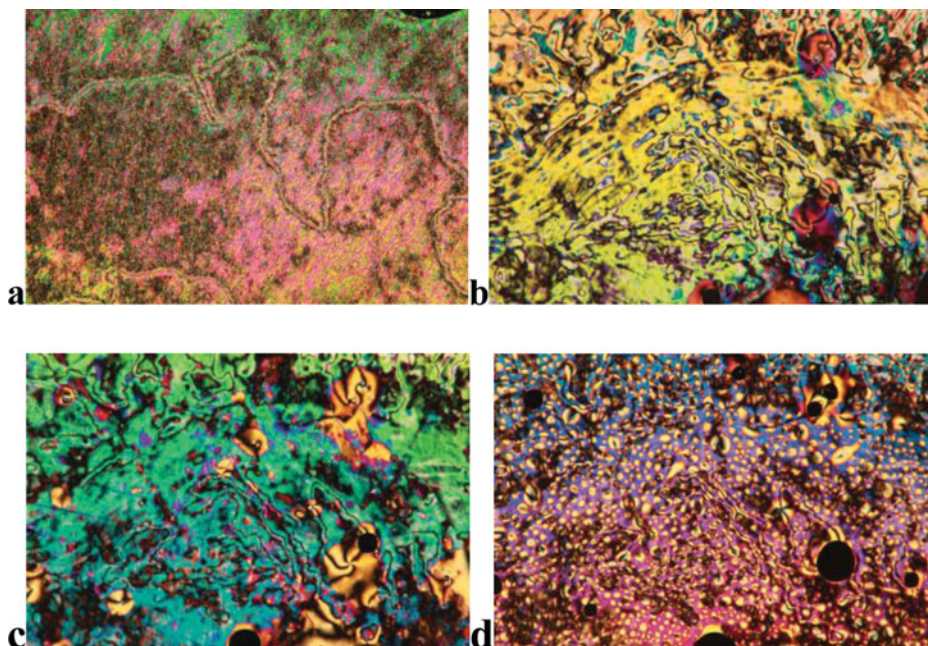


Figure 3. Phase transition of mixture with composition of 33% **8OBAC**. (a) 125°C; (b) 140°C; (c) 145°C; and (d) 149°C.

to an equimolar ratio. It is also obvious that the enthalpy of melting from crystalline phase to liquid crystal for samples in a concentration range of 30–70% of **8OBA** is much lower than that at concentrations close to end members. Change in crystalline structure has a huge impact on the behavior of mixture in mesophase. No significant differences in thermal effects are observed for other phase transitions of the first order as well $Sm \rightarrow N$ as $N \rightarrow I$. Enthalpies of phase transitions are 1 and 3 kJ/mol, respectively. Increase in the region of existence of smectic and nematic phases is observed in the entire range of compositions in the system. The nematic solution is formed by eutectic reaction $\alpha + Sm \rightarrow N$ at an interaction of solid and smectic solutions. The two-phase equilibrium $\alpha + N$ and $\alpha + Sm$ spans range between 3°C and 5°C. At the same time, the range of two-phase equilibrium area $\gamma + Sm$ and $\beta + Sm$ do not exceed 1–2°C. Mixtures showed unusual change in textures in nematic region in a concentration range of 30–70% of **8OBA** (Figs. 3a–d). These texture changes may indicate

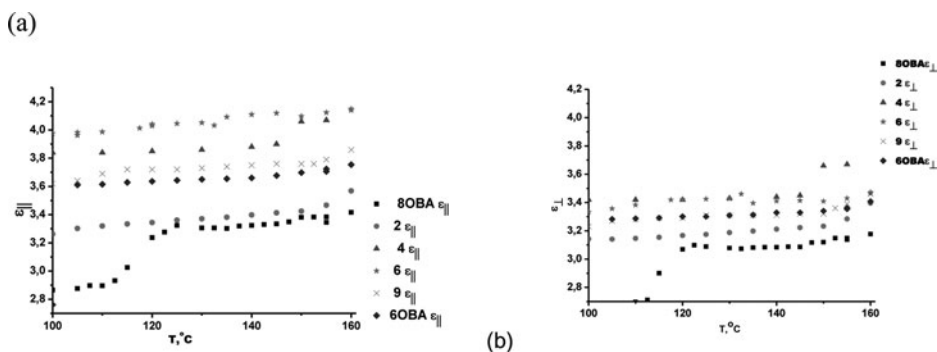


Figure 4. Temperature dependences of (a) longitudinal $\epsilon_{||}$, and (b) transverse ϵ_{\perp} dielectric susceptibilities at various weight proportions between materials.

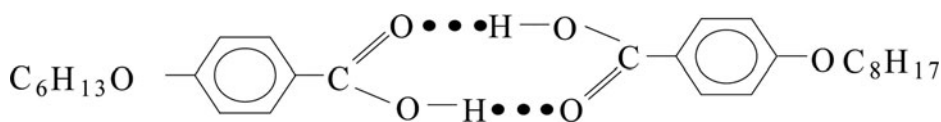


Figure 5. Cross dimer comprising dissimilar monomers **6OBA** and **8OBA**.

several reorientations of molecules in nematic phase because of breaking of hydrogen bonds. This is possible due to difference between molecular structure of mixtures in this area in the crystalline phase and other samples.

4. Dielectric Properties of the System

Here we present our results of dielectric permittivity measurements in mixtures of **6OBA** and **8OBA**.

The temperature dependences of quasi-static values ε_{\parallel} and ε_{\perp} are shown in Figs. 4(a) and (b).

For both pure materials **6OBA** and **8OBA**, the dielectric anisotropy demonstrates small positive values in the whole range of nematic phase.

Detailed analysis of longitudinal and transverse dielectric susceptibilities shows that only the longitudinal contribution is essentially different, while the transverse contribution in the nematic phase is almost the same for each proportion of components. It is natural to suppose that a number of monomers in the mixtures of **6OBA** and **8OBA** tend to combine in cross dimers (comprising dissimilar monomers).

In this case, the small value of longitudinal dielectric susceptibility (and consequently the negative dielectric anisotropy) can originate from the lower longitudinal polarizability of cross dimers (Fig. 5).

For comparison, the value of dielectric anisotropy $\Delta\varepsilon$ as a function of **6OBA** content at reduced temperature ($T_{\text{reduced}} = T_{\text{measurement}} - T_{\text{melting}}$) is shown in Fig. 5.

Notably, dielectric permittivity of equimolar mixture is higher than that for initial components. Increasing the dielectric permittivity for this mixture can be explained by the growth of dipole moment, in which the mixed dimers predominate in comparison to **6OBA** and **8OBA**.

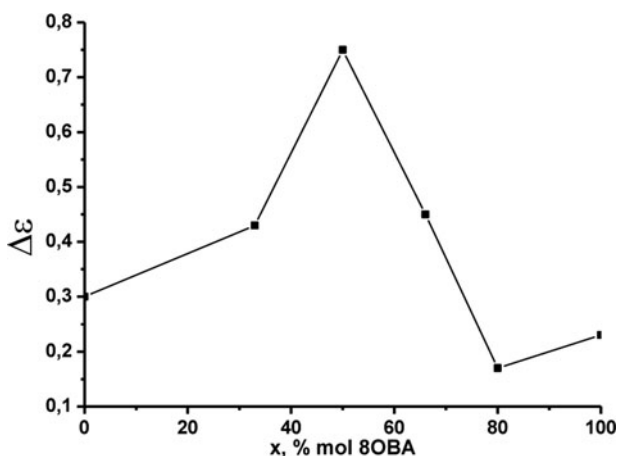


Figure 6. Concentration dependences of dielectric anisotropy $\Delta\varepsilon$ at $T_{\text{reduced}} = -25$ in nematic phase.

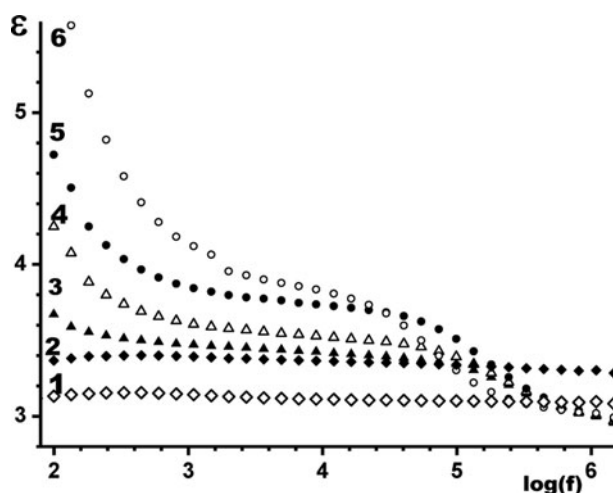


Figure 7. The dependence of dielectric permittivity for the frequency of applied electric field for a sample of 50% mol **8OBA**. (1) 80°C (Sm); (2) 130°C (N); (3) 145°C; (4) 145.5°C; (5) 146°C; and (6) 147°C.

The data obtained make it possible to expect that new structural units – mixed dimers (associates) – are formed in mixtures with a fraction proportion of 30 to 70% mol **8OBA** at melting. For the composition of 80% mol **8OBA**, a number of mixed dimers are obviously not as great as in the range of existence of γ . It is not enough to increase the dipole moment of the system. However, the number of mixed dimers would be enough to break the molecular packing of **6OBA**. This allows us to conclude that the formation of co-crystals takes place for equimolar mixture.

Values of ε_{II} and ε_{\perp} are small, which indicate low polarity dimers of AOBa. The quasi-static values of both ε_{II} and ε_{\perp} are increased with rise in temperature. It is not typical for most of the known liquid crystals and liquid dielectrics. The permittivity should decrease with increasing temperature due to reduction in the degree of orientation of liquid crystal and reduce the density of substance [26]. Increasing ε_{II} and ε_{\perp} can explain growth in the polarity of structural elements involved in the dielectric polarization of AOBa. Dispersion ε_{II} (Fig. 6, lines 3–6) can be a convincing evidence of above-mentioned manifestation at temperatures close to the phase transition of nematic phase – isotropic liquid. It is caused by an exception of orientation contribution from dielectric polarization associated with the rotation of polar molecules around short molecular axes. Usually dispersion of liquid crystals is observed at low temperatures, and disappears with increasing ambient temperature. In contrast, dispersion ε_{III} is absent at a low frequency range of electric field temperatures in nematic and smectic phases for mixtures (Fig. 7, lines 1 and 2). Therefore, increasing the temperature of nematic phase leads to the growth of number of polar structural elements. In addition, it is possible to form new elements and the appearance of polar orientation polarization resulting in increase of dielectric polarization and dielectric constant. Mechanism of formation of polar structural elements is caused by breaking of hydrogen bonds in dimers of AOBa. These phenomena may increase the number of molecules in a substance whose polarity is much higher than the polarity of dimers. It is not excluded in the occurrence of trimmers, in which the dipole moment is greater than the dipole moment of dimer.

5. Conclusions

The present study provides insight into the structure–property relationship of hydrogen-bonded liquid crystals. The phase diagram of two similar mesogens was obtained by POM and DSC. We assume the formation of co-crystal γ at an equimolar ratio. Region of tilted SmC, N phase significantly increases in the range of existence of γ . This may be due to various molecular reorientations and the formation of new associates by hydrogen bonding. For equimolar mixture is observed increasing the dielectric permittivity in comparison with the initial components. So the left side of dipole moment is not fully compensated by the dipole moment of right side in these dimers, which increases the dipole moment of entire system. Increase of dielectric permittivity can be explained by the growth of dipole moment because of predominate mixed dimers in comparison to **6OBA** and **8OBA**. Based on our works, we can conclude that formation of a crystal or compound at a ratio of 1:1 is preferably for a similar length of homologues such as **6OBA–8OBA** and **6OBA–7OBA**, but for acids differing by more than two atoms of C, new components for the future practical use are formed mainly in a ratio of 2:1. The correct ratio of components in the stage of LCD creation should be considered when making precursor compounds with the stable phases of LCD without polymorphic transitions that complicate the introduction of components for practical use.

This model can be used to predict suitability for the creation of other precursors of homologues of carboxylic acids. The advantage of such mixtures, which are co-crystals or compounds of pure components, is the fact that they have a wider range of mesophase existence, and lack of polymorphic transitions hinders their use for further application because of the complexity of thermodynamic calculations and obtaining stable and not super cooled mixtures. Intermolecular interaction has a decisive influence on the physicochemical properties of the system.

References

- [1] Naoum, M. M., Fahmi, A. A., & Alaasar, M. A. (2008). *Mol. Cryst. Liq. Cryst.*, 482, 57.
- [2] Molochko, V. A., & Pestov, S. M. (2003). *Fazovye Ravnovesiya i Termodinamika Sistem s Zhidkimi Kristallami (Phase Equilibria and Thermodynamics of Systems with Liquid Crystals)*, Mosk. Inst. Tonkoi Khim. Tekhnol.: Moscow, Russia.
- [3] Kalinin, N. V., Emelyanenko, A. V., Nosikova, L. A., & Kudryashova, Z. A. (2013). *Phys. Rev.*, E87, 062502.
- [4] Pongali Sathya Prabu, N., & Madhu Mohan, M. L. N. (2013). *Phase Trans.*, 86, 339.
- [5] Vijayakumar, V. N., Murugadass K., & Madhu Mohan, M. L. N. (2010). *Mol. Cryst. Liq. Cryst.*, 517, 43.
- [6] Chitravel T., & Madhu Mohan, M. L. N. (2010). *Mol. Cryst. Liq. Cryst.*, 524, 131.
- [7] Vijayakumar, V. N., & Madhu Mohan, M. L. N. (2009). *Integr. Ferroelectr.*, 392, 81.
- [8] Vijayakumar, V. N., & Madhu Mohan, M. L. N. (2010). *Mol. Cryst. Liq. Cryst.*, 517, 113.
- [9] Vijayakumar, V. N., & Madhu Mohan, M. L. N. (2009). *J. Opt. Elec. Adv. Mater.*, 11, 1139.
- [10] Vijayakumar, V. N., & Madhu Mohan, M. L. N. (2009). *Braz. J. Phys.*, 39, 677.
- [11] Indekeu, J. O., & Berker, A. N. (1988). *J. Phys. France*, 49, 353.
- [12] Imrie, C. T., & Henderson, P. A. (2007). *Chem. Soc. Rev.*, 36, 2096.
- [13] Vijayakumar, V. N., & Madhu Mohan, M. L. N. (2010). *Mol. Cryst. Liq. Cryst.*, 517, 113.
- [14] Vijayakumar, V. N., Mugugadass, K., & Madhu Mohan, M. L. N. (2010). *Mol. Cryst. Liq. Cryst.*, 517, 43.
- [15] Chitravel, T., & Madhu Mohan, M. L. N. (2010). *Mol. Cryst. Liq. Cryst.*, 524, 131.
- [16] Chen, R. H. (2011). *Liquid Crystal Displays: Fundamental Physics and Technology*, Chapter 6, John Wiley: New York, NY.
- [17] Sirbu, S. A., Kudryashova, Z. A., & Nosikova, L. A., (2009). *Liq. Cryst. Their Appl.*, 29(3), 48.

- [18] Kudryashova, Z. A., Nosikova, L. A., Iskhakova, L. D., & Sirbu, S. A. (2008). *Rus. J. Phys. Chem. A.*, 8212, 2065.
- [19] Efremova, E. I., Sirbu, S. A., Kudryashova, Z. A., & Nosikova, L. A. (2013). *Liq. Cryst. Their Appl.*, 44(2), 95.
- [20] Efremova, E. I., & Sirbu, S. A. (2013). In: *Organic and Hybrid Nanomaterials: Trends and Prospects*, Chapter 8, Ivanovo State University, Ministry of Education and Science of the Russian Federation, Russian Foundation for Basic Research: Moscow, Russia, 281 pp.
- [21] Efremova, E. I., Shiryayev, A. A., Sirbu, S. A., Kudryashova, Z. A., Nosikova, L. A., et al. (2015). *Phase Trans.*, 88, 5.
- [22] Dunmur, D., & Toriyama, K. (1999). In: *Physical Properties of Liquid Crystals*, Demus, D., Ed.; Wiley-VCH Verlag GmbH: Weinheim, Germany, 129–150.
- [23] Dierking, I. (2003). *Textures of Liquid Crystals*, Wiley-VCH Verlag GmbH: KGaA, Germany.
- [24] Javadian, S., Dalir, N., & Ghanadzadeh, G. (2015). *J. Chem. Thermodyn.*, 80, 22.
- [25] Rai, U., & Pandey, P. (2003). *Cryst. Growth*, 249, 301.
- [26] Ryumtsev, E. I., Polushin, S. G., & Kovshik, A. P. (1979). *Crystallography*, 24, 547.